nature
structural biology

© 2003 Nature Publishing Group http://www.nature.com/naturestructuralbiology

Seeded conversion of recombinant prion protein to a disulfide-bonded oligomer by a reduction-oxidation process

Sangho Lee & David Eisenberg

The infectious form of prion protein, PrP^{Sc}, self-propagates by its conversion of the normal, cellular prion protein molecule PrP^{C} to another PrP^{Sc} molecule. It has not yet been demonstrated that recombinant prion protein can convert prion protein molecules from PrP^{C} to PrP^{Sc}. Here we show that recombinant hamster prion protein is converted to a second form, PrP^{RDX}, by a redox process *in vitro* and that this PrP^{RDX} form seeds the conversion of other PrP^{C} molecules to the PrP^{RDX} form. The converted form shows properties of oligomerization and seeded conversion that are characteristic of PrP^{Sc}. We also find that the oligomerization can be reversed *in vitro*. X-ray fiber diffraction suggests an amyloid-like structure for the oligomerized prion protein. A domain-swapping model involving intermolecular disulfide bonds can account for the stability and coexistence of two molecular forms of prion protein and the capacity of the second form for self-propagation.

Transmissible spongiform encephalopathies, including bovine spongiform encephalopathy and human Creutzfeldt-Jakob disease[1], are fatal neurodegenerative diseases. The protein-only hypothesis[2] holds that prion proteins are the infectious agents of transmissible spongiform encephalopathies. Two molecular forms of the prion protein, the infectious form (PrP^{Sc}) and the normal cellular form (PrP^{C}), are believed to differ only by their conformations[1]. PrP^{Sc} has been found to differ from PrP^{C} by infectivity, an increased β-sheet content, an increased resistance to proteinase K and an oligomeric state rather than a monomeric state[1].

Mature mammalian prion proteins are molecules of ~209 residues with one conserved disulfide bond between Cys179 and Cys214 (human PrP numbering)[1]. Structures have been determined by NMR in solution for recombinant PrP^{C} from human[3], cow[4], mouse[5] and hamster[6]. All have the same basic monomeric structure, consisting of three α-helices and two strands of β-sheet, with a single disulfide bond bridging helices 2 and 3. In contrast, a crystal structure for recombinant human prion protein revealed a three-dimensional domain-swapped dimer[7], in which a hinge loop (residues 188–195) is changed in conformation from the NMR structure, permitting the C-terminal helix to swap into the second monomer, taking the place of its C-terminal helix, which is then swapped into the core domain of the first monomer. Because in monomeric PrP^{C} the disulfide bond formed by Cys179 and Cys214 links helix 2 to helix 3, conversion of the monomer to the three-dimensional domain-swapped dimer necessitates reduction of the disulfide bond of the monomer and reoxidation in the dimer, now with each Cys179 bonded to Cys214 of the other monomer.

The conversion of PrP^{C} to a second form of prion protein was demonstrated in a cell-free system by Caughey and co-workers by adding scrapie-infected brain extracts to PrP^{C} (ref. 8). The second form was observed to be aggregated and resistant to proteinase K, as is PrP^{Sc}. Conversion required ~1 part of purified PrP^{Sc} from the scrapie-infected hamster brain to 50 parts of PrP^{C} and was found to be more efficient in the presence of 3 M guanidine hydrochloride[9]. Of course, conversion of PrP^{C} to PrP^{Sc} in a cell-free system does not constitute proof of the protein-only hypothesis, because with current analytic tools, one cannot be certain that small amounts of some other infectious agent are not transferred with the 'pure' PrP^{Sc}. A possible role for a sulfhydryl-disulfide exchange reaction during the conversion of PrP^{C} to PrP^{Sc} has been hypothesized[10,11] but so far, experiments have not implicated disulfide-bonded polymers in the conversion of PrP^{C} to PrP^{Sc} (refs. 12,13). Given the possible role for a sulfhydryl-disulfide exchange reaction in the conversion of PrP^{C} to PrP^{Sc} and the domain-swapped crystal structure of a prion protein by disulfide bond exchange, we developed an *in vitro* redox process in which recombinant PrP^{C} can be converted to a second form sharing features of PrP^{Sc}.

RESULTS

Characterization of recombinant hamster PrPs

Our two constructs of recombinant hamster prion protein, termed HisPrP(23–231) and HisPrP(90–231), were expressed in *Escherichia coli* and lack covalent modification, but each contains an N-terminal His-tag for ease of purification. Although the constructs are of different lengths, both span the residues known to be essential for infec-

Howard Hughes Medical Institute, Molecular Biology Institute, UCLA-DOE Institute for Genomics and Proteomics and Department of Chemistry and Biochemistry, University of California, Los Angeles, Los Angeles, California 90095-1570, USA. Correspondence should be addressed to D.E. (david@mbi.ucla.edu).

Published online 3 August 2003; doi:10.1038/nsb961

© 2003 Nature Publishing Group http://www.nature.com/naturestructuralbiology

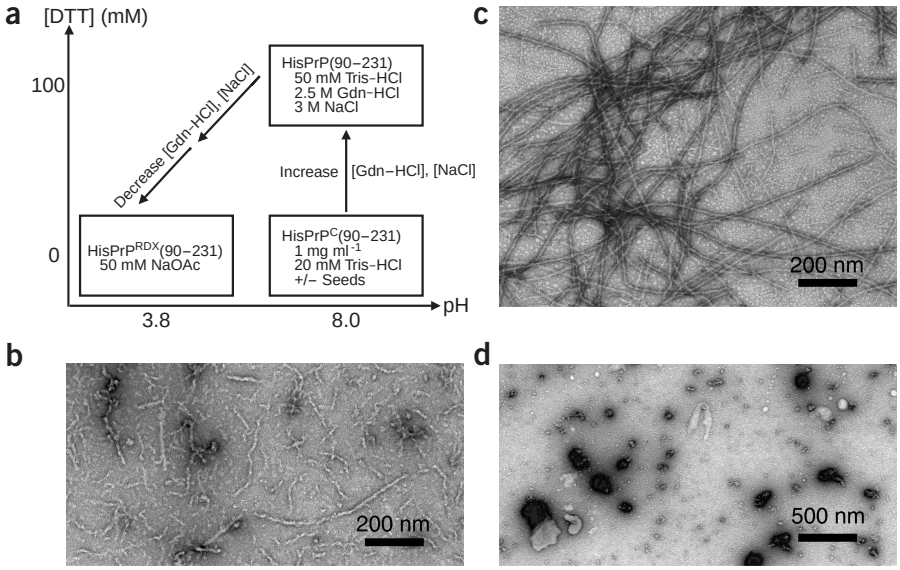

Figure 1 Conversion of the monomeric HisPrP(90–231) to an oligomeric form by a redox process. (**a**) Schematic diagram of the conversion. First, the disulfide bond of HisPrP(90–231) is reduced by DTT at mildly alkaline pH in the presence of high salt and guanidine hydrochloride. In the two steps represented by the solid arrows sloping to the lower left, DTT, salt and guanidine hydrochloride are removed, the pH is reduced and air oxidation of disulfide bonds is permitted. (**b**–**d**) Electron micrographs showing the oligomeric form of HisPrP(90–231) after the redox process. (**b**) Oligomers at completion of the redox process. We term this material unseeded PrP^{RDX}. (**c**) Oligomers at completion of the redox process in which the initial solution has been seeded with the oligomers from **b** (ratio of PrP^{RDX} seeds to PrP^{C} is 1:10). We term this material seeded PrP^{RDX}. (**d**) Aggregates at completion of the redox process without DTT. The processes in **b** and **c** yield an amyloid-like morphology, with the seeded fibrils of **c** being longer, more regular and better defined by negative staining. Only amorphous aggregates are observed in **d** when there is no reduction. Seeds are ~0.1 μg or ~10 μg quantities of PrP^{RDX} prepared by the redox process of **a** and introduced for a second round. Gdn-HCl, guanidine hydrochloride; NaOAc, sodium acetate.

tion[14]. We found both of these recombinant proteins to be monomers in solution by dynamic light scattering, analytical ultracentrifugation and size-exclusion chromatography. Furthermore, they have characteristics of PrP^{C} such as circular dichroism spectra showing α-helical content and sensitivity to proteinase K digestion (data not shown).

A redox process converts recombinant PrP^{C}

Our method for conversion of prion protein requires only purified recombinant PrP^{C} and common chemicals; neither infected brain extracts nor PrP^{Sc} is used. Our process starts by reduction of the conserved disulfide bond at mildly alkaline pH in the presence of high salt and moderate guanidine hydrochloride, followed by lowering the pH to a mildly acidic pH as salt, denaturant and reducing agent are removed (**Fig. 1**). As spontaneous air reoxidation occurs, the disulfide bond reforms. This process differs from earlier protocols reported to convert prion protein *in vitro*[15,16], which were not claimed to seed the conversion of other prion protein molecules. Native gel analysis shows that our converted form is an oligomer (**Fig. 2a**, lanes 2–5, top band). Omission of reducing agent (**Fig. 1d**) or high salt (**Fig. 3a**) from our method prevented conversion, and addition of the alkylating agent iodoacetamide, which reacts with free sulfhydryl groups, preserved most prion protein in the monomeric form (**Fig. 2a**, lane 3). This suggests that the converted form is oligomerized through intermolecular disulfide bonds, and this hypothesis is reinforced by the resolubilization of the oligomer by heating at 95 °C in 125 mM β-mercaptoethanol or DTT (**Fig. 2b**, lanes 3, 4, 6 and 7). Because oligomerization occurs during a reduction-oxidation process, we termed the converted form PrP^{RDX}. Heating oligomerized prion protein without these reducing agents did not appreciably reverse oligomerization (**Fig. 2b**, lane 5). Small amounts of prion protein had apparent dimeric and trimeric molecular masses (**Fig. 2b**, lane 2), also reinforcing our hypothesis of oligomerization of prion protein through intermolecular disulfide bonds. Confirming an earlier study[13], we found that the alkylating agents *N*-ethylmaleimide (**Fig. 2a**, lane 4) and 2-aminoethyl methanethiosulfonate (**Fig. 2a**, lane 5) did not block the conversion process, perhaps because those reagents cannot gain access to the buried cysteine residues[17]. The requirement for the conversion of reducing agent along with high salt and mild denaturant shows that both noncovalent and covalent bonds are broken in conversion. This *in vitro* conversion of PrP^{C} to a second

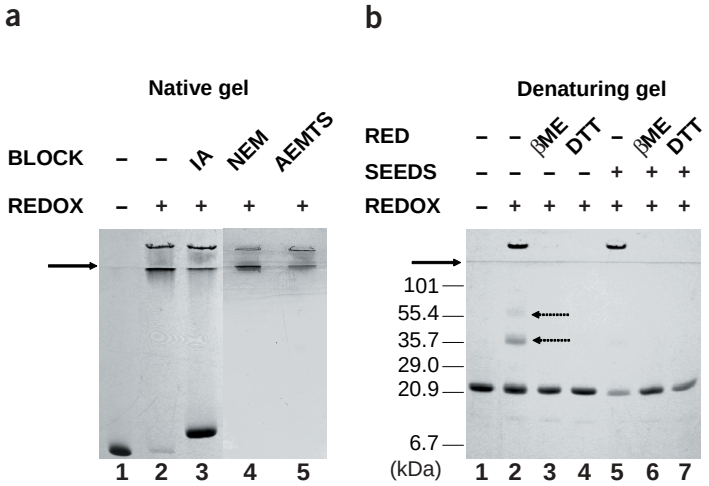

Figure 2 Conversion of PrP^{C} to PrP^{RDX} by intermolecular disulfide linkage. (**a**) Polyacrylamide gradient native gel (4–15%) showing conversion of HisPrP(90–231) (lane 1) to a disulfide-bonded oligomer (lane 2, top band) by the redox process (REDOX) of **Figure 1a**, and its partial prevention by a blocking agent (BLOCK), iodoacetamide (IA) (lane 3). Reduced, iodoacetamide-treated HisPrP(90–231) runs more slowly than control HisPrP(90–231), presumably because its intramolecular disulfide bond is broken. *N*-ethylmaleimide (NEM) and 2-aminoethyl methanethiosulfonate (AEMTS) do not show any prevention (lanes 4 and 5). (**b**) Polyacrylamide SDS gel (20%) showing reversal of conversion of disulfide-bonded oligomer (lane 2) by heating in presence of a reducing agent (RED), either β-mercaptoethanol (βME; lane 3) or DTT (lane 4). Intermolecularly disulfide-bonded dimeric and trimeric prion protein bands are indicated by dashed arrows in lane 2. Seeded oligomerization (lane 5) was reversed in the same way (lanes 6 and 7). Here and in **Figure 3**, the solid arrow shows the boundary between the stacking gel and the running gel. PrP^{RDX} is seen in the stacking gel. The species at the boundary in **Figure 2a** seems to be a noncovalent oligomer, which converts to monomer in denaturing gels (**Fig. 2a**, lane 2 vs. **Fig. 2b**, lane 2).

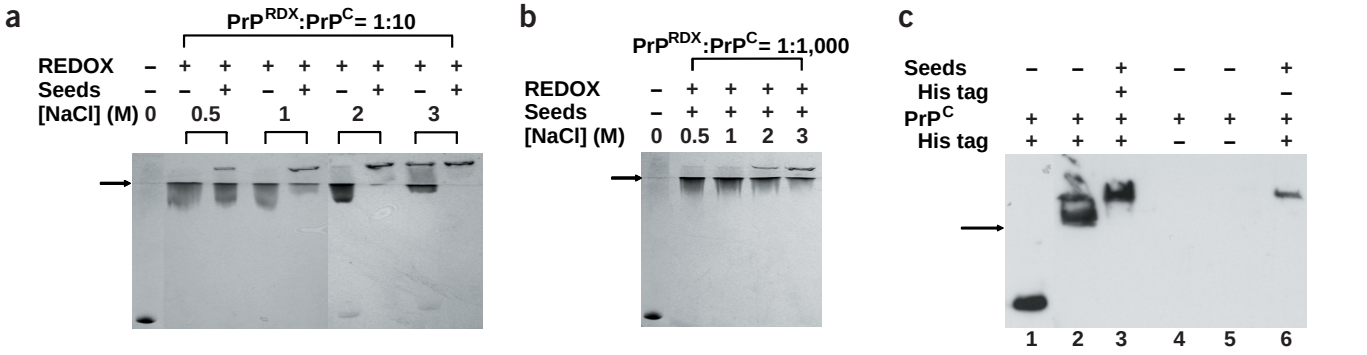

Figure 3 Seeded oligomerization of HisPrP(90–231) by the redox process. (**a**) Ratio of PrP^{RDX} seeds to PrP^{C} is 1:10. (**b**) Ratio of PrP^{RDX} seeds to PrP^{C} is 1:1,000. Oligomerization of HisPrP(90–231) was assayed by the appearance of stalled bands in stacking gel in native gel electrophoresis after the redox process in presence of PrP^{RDX} seeds. Notice that seeded oligomerization requires high salt at the reduction step. Controls without the redox process (REDOX) are shown. (**c**) Incorporation of new PrP^{C} to PrP^{RDX} seeds is shown by immunoblotting using anti-His. Samples were separated in native gels and immunoblotted. HisPrP(90–231) (lane 1) was converted to PrP^{RDX} without seeds (lane 2) and with seeds (lane 3). The N-terminal His-tag of HisPrP(90–231) was cleaved by thrombin (lane 4). PrP^{RDX} seeds were prepared with PrP^{C} without the His-tag (lane 5). PrP^{C} with the His-tag is incorporated to PrP^{RDX} seeds made from PrP^{C} without the His-tag (lane 6).

form does not require other cellular proteins or factors, and is driven instead by concentrations of salt, reducing agent and denaturant far above physiological conditions.

PrP^{RDX} can seed the conversion of PrP^{C} to PrP^{RDX}

PrP^{RDX} seeded the conversion of additional PrP^{C} to PrP^{RDX} (**Fig. 3**). No conversion of PrP^{C} to PrP^{RDX} occurred at salt concentrations <2 M without PrP^{RDX} seeds (**Fig. 3a**), but when seeds of PrP^{RDX} were introduced, conversion occurred at 0.5 M salt and at 2 M even when the ratio of PrP^{RDX} seeds to PrP^{C} was 1:1,000 (**Fig. 3b**). Comparing this ratio to the ratio of 1:50 for PrP^{Sc}:PrP^{C} in the cell-free conversion system[8] suggests that our *in vitro* seeding process is highly effective for conversion. Electron micrographs confirm that seeding increases the yield of amyloid-like PrP^{RDX} fibrils (**Fig. 1b** vs. **Fig. 1c**), and that the seeded fibrils tend to be longer and straighter. Similar results were obtained using HisPrP(23–231) (data not shown). We confirmed the formation of new fibrils by seeding by immunoblotting using monoclonal anti-His (**Fig. 3c**). The antibody did not recognize seeds consisting of PrP^{RDX} without the His-tag (lane 5). However, when PrP^{C}(90–231) with the N-terminal His-tag underwent the redox process in the presence of the same seeds, anti-His detected PrP^{RDX} (lane 6). That is, PrP^{RDX} seeds initiate the conversion of PrP^{C} to new PrP^{RDX} similarly to how PrP^{Sc} in the cell free conversion system[8] initiates conversion of PrP^{C} to new PrP^{Sc}.

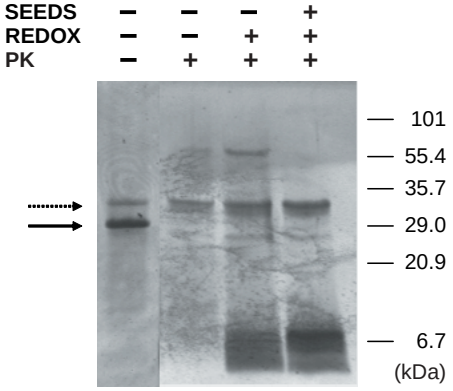

PrP^{RDX} has similarities to PrP^{Sc}

PrP^{RDX} generated by the redox process shows biophysical and biochemical characteristics reminiscent of PrP^{Sc}. We found, from circular dichroism spectroscopy with *g*-factor analysis[18], that the β-sheet content of $HisPrP^{RDX}$(90–231) doubled during conversion from PrP^{C} (from 10% to 20%); this is similar to the increase in β-sheet content during the conversion of PrP^{C} to PrP^{Sc} (ref. 19). PrP^{RDX} was partially resistant to proteinase K digestion (**Fig. 4**), although the transient digestion band with a molecular mass of ~19 kDa, characteristic of PrP^{Sc}, was not observed during $HisPrP^{RDX}$(23–231) digestion. X-ray diffraction of PrP^{RDX} fibrils exhibited a cross-β pattern with a reflection around 4.7-Å resolution, characteristic of anti-parallel β-sheet, and a diffuse reflection with maximum around 11-Å resolution (**Fig. 5**). These suggest an amyloid-like structure containing at least two anti-parallel β-sheets, separated by ~11 Å, formed from strands 4.7 Å apart.

In summary, PrP^{RDX} shares several characteristics of PrP^{Sc}. Like PrP^{Sc} (ref. 20), PrP^{RDX} seeds the conversion of PrP^{C} to a second form. Like PrP^{Sc} (ref. 21), PrP^{RDX} tends to oligomerize in a form with enhanced β-sheet content[19]. Like PrP^{Sc} (refs. 22,23), PrP^{RDX} is resistant to proteolysis by proteinase K, although the commonly observed transient ~19-kDa band was not observed in our experiments. We do not know whether PrP^{RDX} is infectious, that is, whether it can cause prion disease in hamsters.

DISCUSSION

Domain-swapping models for the conversion of PrP

Any acceptable molecular model for the conversion of PrP^{C} to PrP^{Sc} must account for two puzzling features of prions: (i) the stability of PrP^{C} and PrP^{Sc} over long periods of time and yet the rapid conversion between two forms in the presence of a catalytic amount of PrP^{Sc}; and (ii) the templating or infective feature of PrP^{Sc}, which can recruit PrP^{C} molecules into new PrP^{Sc}.

Figure 4 Partial proteinase K (PK) resistance of $HisPrP^{RDX}$(23–231). $HisPrP^{C}$ (23–231) (lane 2) and $HisPrP^{RDX}$(23–231) (~10 μg of each) without (lane 3) and with seeds (lane 4) were digested with proteinase K (50 μg ml^{-1}) in the presence of 1 M Gdn-HCl and 50 mM DTT at 37 °C for 1 h. $HisPrP^{C}$(23–231) without digestion is shown by a line arrow (lane 1). The proteinase K band is indicated by a dashed arrow.

© 2003 Nature Publishing Group http://www.nature.com/naturestructuralbiology

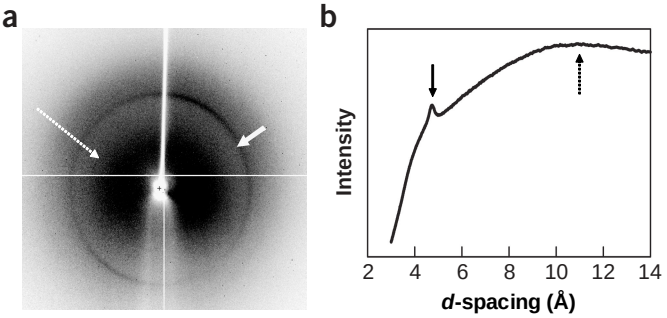

Figure 5 Structural features of HisPrP^{RDX}(90–231). (**a**) X-ray diffraction pattern of seeded HisPrP^{RDX}(90–231). (**b**) Radial profile of the diffraction pattern of **a**. Arrows indicate a reflection peak at 4.7 Å (solid) and the diffuse reflection around 11 Å (dashed).

Oligomeric models involving three-dimensional domain swapping can account for the stability and templating features of prions[24,25] and seem worth considering, given the finding of a domain-swapped dimeric form of human prion protein[7]. The stability of the oligomer depends in part on breaking the intramolecular disulfide bond and reforming an intermolecular disulfide bond (**Fig. 6**). Consider the problem of opening the monomeric PrP^{C} by reduction (**Fig. 6**, upper right) and reforming the intermolecularly disulfide-bonded, domain-swapped dimer (**Fig. 6**, upper left) or the more complex domain-swapped fibril (**Fig. 6**, lower left). The open monomer is unstable because both its covalent disulfide bond and noncovalent interactions must be broken[24]. But when a small amount of free sulfhydryl is introduced into solution at mildly alkaline pH, sulfhydryl-disulfide interchange is promoted[10] and the two forms become interchangeable. In our *in vitro* reduction-oxidation process (**Fig. 1a**), guanidine hydrochloride may facilitate the breaking of interdomain noncovalent interactions and salt in the molar concentration range may enhance domain swapping[26]. Once the noncovalent bonds between helix 3 and the core domain are broken, there are many sources of sulfhydryl groups in cells, including other proteins and glutathione, which could catalyze exchange between PrP^{C} and PrP^{RDX} or PrP^{Sc}. In short, a domain-swapping model accounts for a high kinetic energy barrier that permits two forms of the prion protein to exist in cells, and our observation that disulfide bonding is part of this barrier explains how disulfide interchange might catalyze the exchange.

A domain-swapping model also illuminates the puzzling ability of PrP^{Sc} to convert PrP^{C} to PrP^{Sc}, which has long been discussed in terms of nucleation and crystallization[20,21]. The templating feature of a domain-swapped structure by the formation of a speculative domain-swapped fibril is illustrated (**Fig. 6**, lower left) by a schematic model. Once a monomer has been opened (**Fig. 6**, upper right), the swapping domains (helix 3 and core) are ready to bind to other prion protein molecules, having their complementary domains exposed. The outcome of swapping could be the experimentally observed dimeric prion protein (**Fig. 6**, upper left) in which each helix 3 and core domain bind to the complementary domains on a second molecule. Alternatively, the outcome could be a fibril such as the one illustrated (**Fig. 6**, lower left). In the growing fibril, two free cysteine residues are always extended that can catalyze sulfhydryl-disulfide exchange at the surface of the fibril, opening a new PrP^{C} monomer and rendering it ready to add to the growing, self-complementary fibril.

Figure 6 Speculative model for conversion of PrP^{C} (lower right) to a PrP^{RDX} fibril (lower left). Diagram follows conversion process of **Figure 1a**. PrP^{C} monomer (lower right, PDB entry 1QLX[3]) is opened by guanidine hydrochloride and salt, separating helix 3 from core domain. Cysteine residues, yellow. Monomer is also shown in schematic form, emphasizing disulfide bond between helix 3 and core domain (lower right), and its breaking (upper right). Two open monomers can pair to form a dimer (upper left), as seen in the domain-swapped structure found in the crystalline state[7] (PDB entry 1I4M). Schematic diagram of the domain-swapped dimer emphasizes that helix 3 of the red prion protein (PrP) is swapped into core domain of the blue PrP. Alternatively, a fibril can be formed (lower left). Schematic diagram of PrP^{RDX} fibril emphasizes covalent linkage of PrP molecules building up the fibril, and shows hydrogen bonds as dots, forming the new β-sheet at center of fibril.

Model for the conversion of PrP^{C}

The speculative fibril model for PrP^{RDX} (**Fig. 6**, lower left) is built on an 'open' or 'runaway' domain swap. This is achieved as each new open prion protein molecule joins its helix 3 to the complementary core domain of the prion protein molecule previously added to the growing fibril. Cys214 from the new prion protein molecule forms a disulfide linkage with Cys179 of the previously added prion protein molecule. The hinge loop of the new molecule contributes to the growing β-sheets at the center of the fibril. Circular dichroism spectroscopy shows a doubling in β-sheet content, which is reflected in two new β-sheets. Thus the result of this runaway domain swap is a covalently linked fibril, with a double β-sheet in the center and composite prion protein molecules on the periphery of the cylindrical fibril. Based on the X-ray diffraction pattern (**Fig. 5**), the two sheets are separated by ~11 Å and each is formed from β-strands running perpendicular to the fibril axis, spaced at 4.7 Å. The α-helices of the peripheral domains would not be expected to contribute substantially to the fibril diffraction pattern because these domains are disordered, being linked to the core β-sheets by flexible hinge loops. This expectation is supported by computed diffraction patterns, which have the general character of the observed diffraction pattern (**Fig. 5**). Both the dimer[7] and the PrP^{RDX} fibril contain intermolecular disulfide bonds, in contrast to the PrP^{C} monomer, which has an intramolecular disulfide bond, and in all three types of structure the folding pattern of each PrP molecule is largely preserved.

Conclusions

A redox process converts recombinant PrP^{C} to an oligomeric, protease-resistant higher β-sheet form, PrP^{RDX}. PrP^{RDX} in turn con-

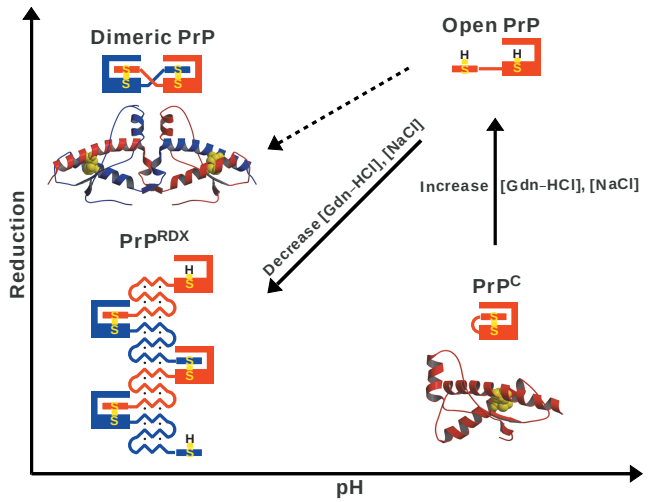

© 2003 Nature Publishing Group http://www.nature.com/naturestructuralbiology

© 2003 Nature Publishing Group http://www.nature.com/naturestructuralbiology

verts other molecules of PrP^{C} to PrP^{RDX}. The redox process and associated controls suggest that formation of intermolecular disulfide bonds is the basis of formation of PrP^{RDX}. These observations and some more general findings on prions can be represented by a domain-swapped structural model in which intermolecular disulfide bonds are formed. Two essential properties of prions are understandable in terms of this covalent domain-swapped model. First, prion protein can exist *in vivo* and *in vitro* for long periods of time in two distinct forms. This ability arises from the high energy barrier to interconversion of the two forms presented by both strong noncovalent and covalent bonds. Second, PrP^{RDX} molecules can recruit new PrP^{C} molecules. The templating feature intrinsic to three-dimensional domain swapping offers a simple mechanism for recruitment of new PrP^{C} molecules to the second form.

METHODS

Plasmid construction. The genes encoding the full-length hamster prion protein and the C-terminal fragment spanning residues 90–231 were amplified by PCR using a plasmid provided by Stefan Weiss at the University of Munich[27]. The amplified genes were cloned into the *Bam*HI and *Eco*RI restriction sites of vector pET28a (Novagen) to produce the plasmids pET28a-PrP(23–231) and pET28a-PrP(90–231), respectively, each of them encoding a fusion protein with a hexahistidine tag at the N terminus of the gene. DNA sequencing confirmed the proper construction of the plasmids.

Protein expression and purification. Plasmids pET28a-PrP(23–231) and pET28a-PrP(90–231) were transformed to *E. coli* BL21(DE3) cells for protein expression. Cells were grown in LB medium with kanamycin at 37 °C. Cells were induced by 1 mM isopropyl β-D-thiogalactopyranoside at $A_{600} = 0.7$ and allowed to grow for an additional 2 h. Cell pellets were resuspended in 50 mM Tris-HCl, pH 8.0, frozen and thawed, and lysed by sonication. The lysed cells were centrifuged at 35,000*g* to separate insoluble from soluble cell fractions. Both HisPrP(23–231) and HisPrP(90–231) were expressed in the insoluble cell fractions. The insoluble fraction was washed extensively with 100 mM Tris-HCl, pH 8.0, followed by 100 mM Tris-HCl, pH 8.0, 0.5% (w/v) tergitol and finally by 1 M NaCl. The washed pellets were dissolved by sonication in dissolving buffer (100 mM Tris-HCl, pH 8.0, 8 M guanidine-HCl, 100 mM DTT). Refolding was performed by rapid dilution in the refolding buffer (100 mM Tris-HCl, pH 7.4, 100 mM glycine, 1.3 M urea, 0.1 mM oxidized glutathione, and 1 mM reduced glutathione) and the resulting solution was stirred at ambient temperature for 1 h and then at 4 °C overnight. The solution was centrifuged to remove precipitates. The precipitates were dissolved in the dissolving buffer for another round of refolding. The soluble, refolded protein from two rounds of refolding was filtered and applied to a HiTrap metal chelating column (Pharmacia) charged with 50 mM nickel sulfate. Protein was eluted with a linear gradient of 50–500 mM imidazole in 20 mM Tris-HCl, pH 8.0, 0.5 M NaCl. Fractions containing pure protein were dialyzed extensively in 20 mM Tris-HCl, pH 8.0, 5 mM EDTA, followed by dialysis in 20 mM Tris-HCl, pH 8.0.

Reduction-oxidation process. Both HisPrP(23–231) and HisPrP(90–231) were subjected to reduction-oxidation process as described (**Fig. 1a**) in three steps. In the first step, protein solution containing either HisPrP(23–231) or HisPrP(90–231) was reduced with 50 mM Tris-HCl, pH 8.0, 100 mM DTT, 2.5 M guanidine-HCl and 3 M NaCl. In the second step, the protein solution was reoxidized in air with 50 mM sodium acetate, pH 3.8 and 1 M guanidine-HCl. The last step was carried out with 50 mM sodium acetate, pH 3.8. Typically, each step was done by dialyzing protein solution at 1 mg ml^{-1} in a volume of 100–150 μl against 300 ml of a buffer containing appropriate chemicals for 16–24 h at 37 °C.

Seeding. Seeds were prepared by the redox process described above. Seeding solution (10 μl) containing either ~10 μg (for PrP^{C}:PrP^{RDX} = 1:10) or ~0.1 μg (for PrP^{C}:PrP^{RDX} = 1:1,000) of the converted form of HisPrP(90–231) was added to the starting solution (**Fig. 1a**, lower right box) in a new round of the redox process. No precipitate was visible in the seeding solution.

Immunoblotting. Samples were separated in 10% or 15% (w/v) polyacrylamide native gel in *N*-tris[hydroxymethyl]methyl-3-aminopropane-sulfonic acid and histidine buffer system using reversed electrodes and transferred to a polyvinylidene fluoride (PVDF) membrane. Monoclonal anti-His (Novagen) was added to the PrP^{RDX} sample with a 1:5,000 dilution. Secondary antibody conjugated with chemiluminescent compounds was added with a 1:1,000 dilution.

Alkylation of free sulfhydryl groups. Each of iodoacetamide, *N*-ethylmaleimide or 2-aminoethyl methanethiosulfonate was added at a final concentration of 150 mM after the initial reduction step of the redox process, at which 50 mM DTT was used in place of 100 mM DTT, and solution was incubated for 6 h at 37 °C before the subsequent steps of the redox process were carried out. To maintain a proper pH of the system during alkylation step, 500 mM Tris-HCl, pH 8.5 for iodoacetamide or 50 mM Tris-HCl, pH 7.0 for *N*-ethylmaleimide was used at the alkylation step of the redox process in place of 50 mM Tris-HCl, pH 8.0.

Proteinase K resistance assay. Proteinase K (Sigma) was dissolved in 0.1 M Tris-HCl, pH 8.0 at 2.5 mg ml^{-1}. HisPrP(23–231) (~10 μg) was digested by proteinase K at a final concentration of 50 μg ml^{-1}. All the tubes were incubated at 37 °C for 1 h. The solutions were inactivated by adding 2 mM PMSF. Samples were methanol-precipitated and analyzed by SDS-PAGE using a 20% (w/v) homogeneous gel (Pharmacia) on PHAST system (Pharmacia).

Native gel electrophoresis. Protein samples were loaded to a 4–15% (w/v) gradient gel (Pharmacia) on PHAST system (Pharmacia). As both HisPrP(23–231) and HisPrP(90–231) are basic proteins, reversed electrodes and gel strips for basic proteins were used according to the manufacturer's manual (Pharmacia).

Electron microscopy. Carbon-coated parlodion support films mounted on copper grids were made hydrophilic immediately before use by high-voltage, alternating current glow discharge. Samples were applied directly onto grids and allowed to adhere for 2 min. Grids were rinsed with distilled water and stained with 1% (w/v) uranyl acetate. Specimens were examined in a Hitachi H-7000 electron microscope at an accelerating voltage of 75 kV.

X-ray diffraction. Seeded $HisPrP^{RDX}$(90–231) (~200 μg) was applied to the ends of capillaries and allowed to dry overnight. Images were recorded at ambient temperature on a Quantum 4 CCD area detector (Area Detector Systems) equipped with a Rigaku FR-D X-ray generator (Molecular Structure).

ACKNOWLEDGMENTS

We thank S.B. Prusiner's laboratory for helping us in fermentation of HisPrP(90–231), M. Gingery for electron microscopy, M.R. Sawaya for building the model of the PrP^{RDX} fibril, R.L. Garrell's laboratory for helping us in *g*-factor analysis, M. Apostol for assistance and P.D. Boyer, T.E. Creighton and A.K. Chamberlain for critical reading of the manuscript. This work was supported by the Howard Hughes Medical Institute and the US National Institutes of Health.

COMPETING INTERESTS STATEMENT

The authors declare that they have no competing financial interests.

Received 9 April; accepted 14 July 2003
Published online at http://www.nature.com/naturestructuralbiology/

1. Prusiner, S.B. Prions. *Proc. Natl. Acad. Sci. USA* **95**, 13363–13383 (1998).
2. Griffith, J.S. Self-replication and scrapie. *Nature* **215**, 1043–1044 (1967).
3. Zahn, R. *et al.* NMR solution structure of the human prion protein. *Proc. Natl. Acad. Sci. USA* **97**, 145–150 (2000).
4. Lopez Garcia, F., Zahn, R., Riek, R. & Wuthrich, K. NMR structure of the bovine prion protein. *Proc. Natl. Acad. Sci. USA* **97**, 8334–8339 (2000).
5. Riek, R. *et al.* NMR structure of the mouse prion protein domain PrP(121–231). *Nature* **382**, 180–182 (1996).
6. James, T.L. *et al.* Solution structure of a 142-residue recombinant prion protein corresponding to the infectious fragment of the scrapie isoform. *Proc. Natl. Acad. Sci. USA* **94**, 10086–10091 (1997).
7. Knaus, K.J. *et al.* Crystal structure of the human prion protein reveals a mechanism for oligomerization. *Nat. Struct. Biol.* **8**, 770–774 (2001).
8. Kocisko, D.A. *et al.* Cell-free formation of protease-resistant prion protein. *Nature* **370**, 471–474 (1994).
9. Horiuchi, M. & Caughey, B. Specific binding of normal prion protein to the scrapie

form via a localized domain initiates its conversion to the protease-resistant state. *EMBO J.* **18**, 3193–3203 (1999).
10. Welker, E., Wedemeyer, W.J. & Scheraga, H.A. A role for intermolecular disulfide bonds in prion diseases? *Proc. Natl. Acad. Sci. USA* **98**, 4334–4336 (2001).
11. Feughelman, M. & Willis, B.K. Thiol-disulfide interchange a potential key to conformational change associated with amyloid fibril formation. *J. Theor. Biol.* **206**, 313–315 (2000).
12. Turk, E., Teplow, D.B., Hood, L.E. & Prusiner, S.B. Purification and properties of the cellular and scrapie hamster prion proteins. *Eur. J. Biochem.* **176**, 21–30 (1988).
13. Welker, E., Raymond, L.D., Scheraga, H.A. & Caughey, B. Intramolecular versus intermolecular disulfide bonds in prion proteins. *J. Biol. Chem.* **277**, 33477–33481 (2002).
14. Prusiner, S.B. *et al.* Further purification and characterization of scrapie prions. *Biochemistry* **21**, 6942–6950 (1982).
15. Jackson, G.S. *et al.* Reversible conversion of monomeric human prion protein between native and fibrilogenic conformations. *Science* **283**, 1935–1937 (1999).
16. Swietnicki, W., Morillas, M., Chen, S.G., Gambetti, P. & Surewicz, W.K. Aggregation and fibrillization of the recombinant human prion protein huPrP90–231. *Biochemistry* **39**, 424–431 (2000).
17. Venkatesan, P., Liu, Z., Hu, Y. & Kaback, H.R. Site-directed sulfhydryl labeling of the lactose permease of *Escherichia coli*: *N*-ethylmaleimide-sensitive face of helix II. *Biochemistry* **39**, 10649–10655 (2000).
18. McPhie, P. Circular dichroism studies on proteins in films and in solution: estimation of secondary structure by *g*-factor analysis. *Anal. Biochem.* **293**, 109–119 (2001).
19. Pan, K.-M. *et al.* Conversion of α-helices into β-sheets features in the formation of the scrapie prion proteins. *Proc. Natl. Acad. Sci. USA* **90**, 10962–10966 (1993).
20. Harper, J.D. & Lansburry, P.T. Models of amyloid seeding in Alzheimer's disease and scrapie: mechanistic truths and physiological consequences of the time-dependent solubility of amyloid proteins. *Annu. Rev. Biochem.* **66**, 385–407 (1997).
21. Caughey, B. Transmissible spongiform encephalopathies, amyloidoses and yeast prions: common threads? *Nat. Med.* **6**, 751–754 (2000).
22. McKinley, M.P., Bolton, D.C. & Prusiner, S.B. A protease-resistant protein is a structural component of the scrapie prion. *Cell* **35**, 57–62 (1983).
23. Caughey, B. *et al.* Normal and scrapie-associated forms of prion protein differ in their sensitivities to phospholipase and proteases in intact neuroblastoma cells. *J. Virol.* **64**, 1093–1101 (1990).
24. Schlunegger, M.P., Bennet, M.J. & Eisenberg, D. Oligomer formation by 3D domain swapping: a model for protein assembly and misassembly. *Adv. Protein Chem.* **50**, 61–122 (1997).
25. Cohen, F.E. Protein misfolding and prion diseases. *J. Mol. Biol.* **293**, 313–320 (1999).
26. Steere, B. & Eisenberg, D. Oligomerization of high-order diphtheria toxin oligomers. *Biochemistry* **39**, 15901–15909 (2000).
27. Weiss, S. *et al.* Overexpression of active Syrian golden hamster prion protein PrPc as a glutathione *S*-transferase fusion in heterologous systems. *J. Virol.* **69**, 4776–4783 (1995).

© 2003 Nature Publishing Group http://www.nature.com/naturestructuralbiology